

Low-frequency hybridized excess vibrations of two-dimensional glasses

Licun Fu(付立存), Yiming Zheng(郑一鸣), and Lijin Wang(王利近)

Citation: Chin. Phys. B, 2024, 33 (**5**): 056401. DOI: 10.1088/1674-1056/ad205e
Journal homepage: http://cpb.iphy.ac.cn; http://iopscience.iop.org/cpb

What follows is a list of articles you may be interested in

Novel structures and mechanical properties of Zr_2N: *Ab initio* description under high pressures

Minru Wen(文敏儒), Xing Xie(谢兴), Zhixun Xie(谢植勋), Huafeng Dong(董华锋), Xin Zhang(张欣), Fugen Wu(吴福根), and Chong-Yu Wang(王崇愚)
Chin. Phys. B, 2021, 30 (**1**): 016403. DOI: 10.1088/1674-1056/abb220

Compression behavior and spectroscopic properties of insensitive explosive 1,3,5-triamino-2,4,6-trinitrobenzene from dispersion-corrected density functional theory

Yan Su(苏艳), Junyu Fan(范俊宇), Zhaoyang Zheng(郑朝阳), Jijun Zhao(赵纪军), Huajie Song(宋华杰)
Chin. Phys. B, 2018, 27 (**5**): 056401. DOI: 10.1088/1674-1056/27/5/056401

Unraveling the effect of uniaxial strain on thermoelectric properties of Mg_2Si: A density functional theory study

Kulwinder Kaur, Ranjan Kumar
Chin. Phys. B, 2017, 26 (**6**): 066401. DOI: 10.1088/1674-1056/26/6/066401

Properties of sound attenuation around a two-dimensional underwater vehicle with a large cavitation number

Ye Peng-Cheng (叶鹏程), Pan Guang (潘光)
Chin. Phys. B, 2015, 24 (**6**): 066401. DOI: 10.1088/1674-1056/24/6/066401

Low-frequency hybridized excess vibrations of two-dimensional glasses

Licun Fu(付立存), Yiming Zheng(郑一鸣), and Lijin Wang(王利近)†

School of Physics and Optoelectronic Engineering, Anhui University, Hefei 230601, *China*

(Received 18 November 2023; revised manuscript received 4 January 2024; accepted manuscript online 19 January 2024)

One hallmark of glasses is the existence of excess vibrational modes at low frequencies ω beyond Debye's prediction. Numerous studies suggest that understanding low-frequency excess vibrations could help gain insight into the anomalous mechanical and thermodynamic properties of glasses. However, there is still intensive debate as to the frequency dependence of the population of low-frequency excess vibrations. In particular, excess modes could hybridize with phonon-like modes and the density of hybridized excess modes has been reported to follow $D_{\rm exc}(\omega) \sim \omega^2$ in 2D glasses with an inverse power law potential. Yet, the universality of the quadratic scaling remains unknown, since recent work suggested that interaction potentials could influence the scaling of the vibrational spectrum. Here, we extend the universality of the quadratic scaling for hybridized excess modes in 2D to glasses with potentials ranging from the purely repulsive soft-core interaction to the hard-core one with both repulsion and attraction as well as to glasses with significant differences in density or interparticle repulsion. Moreover, we observe that the number of hybridized excess modes exhibits a decrease in glasses with higher density or steeper interparticle repulsion, which is accompanied by a suppression of the strength of the sound attenuation. Our results indicate that the density bears some resemblance to the repulsive steepness of the interaction in influencing low-frequency properties.

Keywords: density of states, vibrational modes, sound attenuation, two-dimensional glasses

PACS: 64.70.Q–, 64.70.kj **DOI:** 10.1088/1674-1056/ad205e

1. Introduction

As a typical non-crystalline material, glass exhibits numerous special properties in comparison to those of crystalline solids. According to the classical Debye theory,[1] the low-frequency vibrational density of states of crystals follows $D(\omega) \sim \omega^{d-1}$, where ω and d are the frequency and spatial dimensions, respectively; the specific heat deduced from this conforms to $C(T) \sim T^d$ with T being the temperature.

However, scenarios in glasses are different and complex. The low-frequency spectrum in the density of states of glasses is beyond the Debye prediction. Specifically, low-frequency vibrational modes of glasses are composed of phonon-like modes and excess modes:[2–5] the density of phonon-like modes obeys the Debye density of states, while that of excess modes deviates from the Debye prediction. Consequently, there are significant differences in some low-temperature properties[6–8] between glasses and crystals. For instance, at temperatures near 3 K–10 K in 3D glasses, the reduced specific heat $C(T)/T^3$ exhibits a peak that is suggested to originate from the boson peak referring to the maximum in the reduced density of states $D(\omega)/\omega^2$. Additionally, numerous studies[9–20] over the past few decades have already established compelling connections between properties of excess modes and those of glasses and even glass-forming liquids.

Describing the low-frequency density of excess vibrations $D_{\rm exc}(\omega)$ plays a pivotal role in shedding light on the elusive low-temperature properties of glasses. Although it has long been established that the low-frequency tail of $D_{\rm exc}(\omega)$ goes to zero as a power law ω^γ, the scaling exponent γ is still uncertain. Theoretical studies[21–35] suggest that the value of γ could fall within the range of 2 to 5. For instance, it was proposed in the heterogeneous elasticity theory[28] that $D_{\rm exc}(\omega)$ is proportional to the sound attenuation coefficient whose frequency dependence follows the Rayleigh scattering scaling at low frequencies, thus indicating $D_{\rm exc}(\omega) \sim \omega^{d+1}$.

Computer simulations now play an indispensable role in the investigation of properties pertaining to excess modes. However, phonon-like modes hybridize inevitably with excess modes in large enough systems,[36] which thus poses a great challenge in the numerical determination of γ. In order to probe the low-frequency spectrum contributed by excess modes in the density of states, one has to separate the phonon-like modes and excess modes. There are generally two approaches to this problem.

The first idea is to study specific glasses where excess modes do not hybridize with phonon-like modes. One could reduce the size of the system so that the frequency of the lowest phonon-like mode $\omega_1 = 2\pi\sqrt{G/\rho}/L$ (G is the shear modulus, L is the box length and ρ is the density) could be shifted toward a higher frequency. This thus exposes a low-frequency window below ω_1 where phonon-like modes are not allowed and hence there are only excess modes. A large amount of simulation work[37–50] following this line suggests that γ could depend on the system size,[38,39,41] glass stability,[42,47] spatial

†Corresponding author. E-mail: lijin.wang@ahu.edu.cn

© 2024 Chinese Physical Society and IOP Publishing Ltd

dimensions,[38,45] stress distribution,[29,46] fraction of pinned particles[48,50] or even the frequency range examined.[37,38] However, to date, consensus is still lacking regarding the value of γ in simulations. Here, we refer to Refs. [37–39] for the latest study of the low-frequency spectrum in the density of excess modes not hybridizing with phonon-like modes.

The second idea is to conceive effective ways to distinguish between excess modes and phonon-like modes.[2–5] The hybridization between excess modes and phonon-like modes usually occurs at frequencies around and above the lowest phonon-like mode in large-scale systems. One way proposed to pick out excess modes is to set a threshold of participation ratio p_c, based on the assumption that participation ratios of phonon-like modes are usually greater than those of excess modes.[2] Specifically, those modes with participation ratios exceeding p_c are categorized as phonon-like modes, while the remaining modes are regarded as excess modes. It was reported that the exponent $\gamma = 4$ in 3D glasses when using this classification method, which is independent of the interaction potential model[2–4] or the glass stability.[3] However, this method would not work well in 2D glasses, because γ is found to be sensitive to the choice of p_c[5] and sometimes this method could even lead to the claim that there are no excess modes at low frequencies in large 2D glasses.[2]

Although it still remains challenging to distinguish directly between phonon-like modes and excess modes in 2D glasses as well as in 3D glasses, recent efforts have indicated the feasibility of indirectly obtaining the density of hybridized excess modes. One indirect method is to subtract the Debye part contributed by phonon-like modes from the total density of states, and the remainder is thus the density of hybridized excess modes.[28] This method could lead to $\gamma = 4$ in 3D glasses,[5] which is in line with that achieved through the participation ratio threshold method,[2–4] while it leads to $\gamma = 2$ in 2D glasses.[5] This indicates that the value of γ and hence the density of hybridized excess modes depends on spatial dimensions.

It is worth noting that the quartic frequency dependence of the population of hybridized excess modes in 3D glasses has been extended to various glasses with, e.g., significantly different interaction potentials and preparation histories, thus demonstrating its robustness.[2–5] However, a comprehensive investigation into the universality of the quadratic frequency dependence of the density of hybridized excess modes in 2D glasses is still lacking, though such a dependence has been demonstrated in the inverse power-law potential models with different glass stability in Ref. [5]. We also note that one very recent work[29] suggests that the details of interaction potentials could influence the density of excess modes that do not hybridize with phonon-like modes, which makes the study of the interaction potential dependence of the spectrum of excess modes that hybridize with phonon-like modes imperative.

In this paper, we systematically investigate the density of hybridized excess modes $D_{\rm exc}(\omega)$ in 2D model glass-formers with different classes of interaction potentials. We get $D_{\rm exc}(\omega)$ by subtracting the Debye contribution from the total density of states. In all cases, we could observe $D_{\rm exc}(\omega) = A_2\omega^2$, thus generalizing the quadratic frequency dependence of $D_{\rm exc}(\omega)$ to a wider range of glass-formers. As for the prefactor A_2, it could exhibit variations under different conditions. We mainly probe the dependence of A_2 on the density ρ and the steepness of interparticle repulsion χ in purely repulsive hard-core interaction potential models. We find, with an increase in ρ or χ, A_2 decreases, which is accompanied by a suppression of the sound attenuation.

2. Models and methods

We conducted numerical simulations of vibrational modes in 2D glass-formers with three different interaction potential models. The models include the purely repulsive soft-core harmonic (HARM) potential, the purely repulsive hard-core inverse-power-law (IPL) potential and the generic hard-core Lennard–Jones (LJ) potential with both attractive and repulsive contributions. We refer to the supplementary material of Ref. [5] for simulation details regarding the three interaction potential models. In particular, we tune the power exponent n in the IPL potential $\sim 1/r^n$ with r the interparticle distance, to simulate glasses with different steepness of the interparticle repulsion χ. Thus, χ positively correlates with n. In addition, we change the density $\rho = N/L^2$ by tuning the side length L when the system size N is fixed in the IPL potential model with a fixed $n = 12$. Note that all our results with respect to the density of hybridized excess modes are from systems with the same system size $N = 20000$, whereas results regarding the sound attenuation are from systems with $N = 20000$ and $N = 100000$.

We performed analysis of vibrations of zero-temperature ($T = 0$) glasses (also termed inherent structures), which are generated by a very rapid quench of high-temperature liquids to $T = 0$ through energy minimization. We calculated the Hessian matrix (the second-order partial derivatives of the total potential with respect to particle displacements) of $T = 0$ glasses, and diagonalized the matrix using the Intel math kernel library[51] to obtain eigenvalues and hence corresponding eigenfrequencies. In particular, the l-th eigenvalue λ_l is associated with the l-th eigenfrequency ω_l via $\omega_l = \sqrt{\lambda_l}$.

The total density of states in 2D is given by

$$D(\omega) = \frac{1}{2N-2}\sum_{l=1}^{2N-2}\delta(\omega-\omega_l). \tag{1}$$

To avert the binning issue[5,37,38] encountered frequently in the numerical calculation of $D(\omega)$, we calculate instead the total

cumulative density of states, which reads

$$I(\omega) = \int_0^{\omega} D(\omega')\,\mathrm{d}\omega'. \tag{2}$$

The cumulative density of hybridized excess modes $I_{\rm exc}(\omega)$ is obtained by subtracting the Debye contribution $I_{\rm D}(\omega)$ from the total cumulative density of states, i.e.,

$$I_{\rm exc}(\omega) = I(\omega) - I_{\rm D}(\omega). \tag{3}$$

Here, $I_{\rm D}(\omega) = 1/2A_{\rm D}\omega^2$, and the Debye level $A_{\rm D}$ is determined independently.[2,5]

3. Results

A recent numerical simulation study[5] suggests that the density of hybridized excess modes of 2D glasses with IPL potentials with $n = 12$ follows $I_{\rm exc}(\omega) \sim \omega^3$, regardless of the glass stability. However, the universality of this scaling under different conditions is unchecked. One important factor is the interaction potentials that could underpin some properties of glasses and glass-forming liquids.[14,17,29,52–56] In particular, it has been reported very recently that the scaling exponent in the spectrum of excess modes not hybridizing with phonon-like modes below the first phonon-like mode depends largely on the details of the interaction potentials.[29] This motivates us to check the university of $I_{\rm exc}(\omega) \sim \omega^3$ in different interaction potential models.

We show in Fig. 1 the cumulative density of hybridized excess modes $I_{\rm exc}(\omega)$ in 2D glass-formers with three significantly different but widely used interaction potentials, namely, HARM, IPL and LJ. We also show the corresponding total cumulative density of states $I(\omega)$ in the inset of Fig. 1. It is apparent that the low-frequency tail of $I_{\rm exc}(\omega)$ conforms to the power-law scaling of $I_{\rm exc}(\omega) \sim \omega^3$, i.e., $D_{\rm exc}(\omega) \sim \omega^2$ in each interaction potential model examined here. Therefore, we extend the university of the cubic frequency dependence of $I_{\rm exc}(\omega)$ to more potential models ranging from the hard-core interaction to soft-core interaction as well as from the purely repulsive interaction to the interaction with both repulsion and attraction. However, more work is needed to check the university of this cubic scaling at much lower frequencies and in more complicated interaction potentials.

We next examine how the frequency dependence of $I_{\rm exc}(\omega)$ is influenced by the steepness of the repulsive interaction χ and the system density ρ. We note that χ and ρ have been suggested to have an influence on excess modes not hybriziding with the phonon-like modes below the first phonon-like mode in 3D glasses.[57] However, recent studies[5,29] suggest that the scaling of the density of excess modes depends on whether excess modes hybridize with phonon-like modes and also on spatial dimensions, and hence it may be unsafe to extrapolate the χ (or ρ) dependence of excess modes hybridizing with phonon-like modes in 2D glasses from the χ (or ρ) dependence of excess modes not hybridizing with phonon-likes in 3D glasses. This stimulates us to examine directly how χ and ρ affect $I_{\rm exc}(\omega)$ in 2D glasses, respectively.

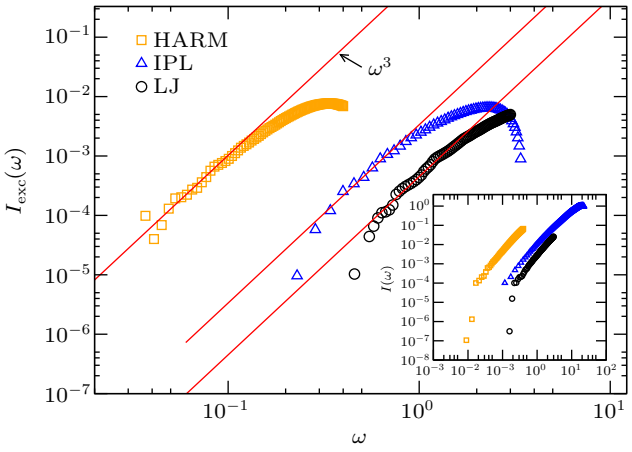


Fig. 1. Cumulative density of hybridized excess modes $I_{\rm exc}(\omega)$ (the main panel) and the corresponding total cumulative density of states $I(\omega)$ (the inset) in 2D model glasses with HARM, IPL ($n = 12$ and $\rho = 1.0$) and LJ potentials. $I_{\rm exc}(\omega)$ is obtained by subtracting the Debye contribution from $I(\omega)$ according to Eq. (3). In all three examined glass-formers, the low-frequency tail of $I_{\rm exc}(\omega)$ conforms to the power-law scaling of $I_{\rm exc}(\omega) \sim \omega^3$ (red lines).

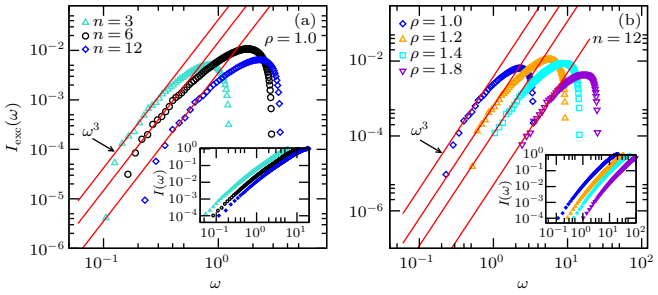


Fig. 2. Cumulative density of hybridized excess modes $I_{\rm exc}(\omega)$ (the main panels) and the corresponding total cumulative density of states $I(\omega)$ (the insets) in 2D model glasses with IPL interaction potentials $\sim 1/r^n$. (a) The same density $\rho = 1.0$ but different n ($n = 3$, $n = 6$ and $n = 12$). (b) The same $n = 12$ but different ρ ($\rho = 1.0$, $\rho = 1.2$, $\rho = 1.4$ and $\rho = 1.8$). A larger value of n corresponds to a steeper repulsion in the interparticle interaction. Each red line represents $I_{\rm exc}(\omega) \sim \omega^3$. Note that the $I(\omega)$ data for each (n, ρ) are obtained from systems with $N = 20000$.

To simulate glasses with different χ, we tune n in the IPL potential $\sim 1/r^n$ at a fixed density ρ, and hence a larger value of n corresponds to a steeper repulsion χ. The χ and ρ dependences of $I_{\rm exc}(\omega)$ are shown in Figs. 2(a) and 2(b), respectively. One could observe that the scaling $I_{\rm exc}(\omega) \sim \omega^3$ works well at low frequencies in all cases, regardless of the density or the steepness of the repulsion, which thus extends further the universality of the cubic scaling. However, it is apparent that the magnitude of $I_{\rm exc}(\omega)$ is sensitive to the change of χ or ρ. Specifically, if we denote A_2 as the prefactor in the power law $I_{\rm exc}(\omega) = 1/3A_2\omega^3$ so that $D_{\rm exc}(\omega) = A_2\omega^2$, one could observe that A_2 exhibits a decrease with an increase in χ or ρ. Therefore, there are fewer hybridized excess modes in denser glasses or in glasses with a steeper repulsion of interaction.

In addition, it can be inferred that there are fewer low-frequency modes (composed of both excess modes and phonon-like modes) in glasses with larger density (or steeper repulsion) when comparing the total cumulative density of excess modes $I(\omega)$ at different ρ with the same χ (or at different χ with the same ρ); see the insets of Figs. 2(a) and 2(b). It is worth noting that $I_{\rm exc}(\omega)$ is obtained by subtracting the Debye contribution from $I(\omega)$, which implies that the change of $I(\omega)$ with ρ (or χ) may not be inferred simply from the change of $I_{\rm exc}(\omega)$ with ρ (or χ) and the other way around.

Moreover, it has been suggested that the transverse sound attenuation is connected with the density of hybridized excess modes in both 2D and 3D glasses.[5,58] Specifically, with an increase of the glass stability, not only are there fewer hybridized excess modes, but also the strength of the transverse sound attenuation is suppressed. It is then natural to check how the transverse sound attenuation evolves with the steepness of interparticle repulsion and the density.

Following the procedure in Ref. [58], we determine the transverse sound attenuation coefficient $\Gamma(\omega)$ and corresponding frequency ω. First, we set the initial velocity of particle i according to $\dot{\boldsymbol{u}}_i(t=0)=\boldsymbol{a}\sin(\boldsymbol{k}\cdot\boldsymbol{r}_i)$, where $\boldsymbol{a}\cdot\boldsymbol{k}=0$, $\boldsymbol{k}$ is the wavevector, $\boldsymbol{a}$ is a unit vector and $\boldsymbol{r}_i$ is the position vector of particle i in the inherent structures. Second, we calculate the velocity correlation function $C(k,t)$ when solving the equation of motion within harmonic approximation. Specifically, the equation of motion reads

$$\ddot{\boldsymbol{u}}_i(t)=\dot{\boldsymbol{u}}_i(t=0)\delta(t)-\sum_{j=1}^{N}D_{ij}\boldsymbol{u}_j(t), \tag{4}$$

where D_{ij} is the dynamic matrix, which is the same as the Hessian matrix since all particles have the same mass $m=1$ in our study, and $\boldsymbol{u}_i(t)$ denotes the displacement of particle i at t from $\boldsymbol{r}_i$. The velocity correlation function under transverse excitation is

$$C(k,t)=\left\langle\frac{\sum_{i=1}^{N}\dot{\boldsymbol{u}}_i(0)\cdot\dot{\boldsymbol{u}}_i(t)}{\sum_{i=1}^{N}\dot{\boldsymbol{u}}_i(0)\cdot\dot{\boldsymbol{u}}_i(0)}\right\rangle. \tag{5}$$

Figure 3(a) shows examples of $C(k,t)$ calculated at two different k. It can be seen that the decay of $C(k,t)$ is faster at a greater k. Ideally, the transverse sound attenuation Γ and the corresponding frequency ω could be obtained by fitting the velocity correlation function to

$$C(k,t)=\exp(-\Gamma t/2)\cos(\omega t). \tag{6}$$

In numerical studies of finite-size systems, this could give an accurate determination of ω but not Γ due to the reported finite-size effect on Γ.[58–61] In particular, as shown in Fig. 3(b), the envelopes of $C(k,t)$, $E(k,t)$ referring to all peaks in $|C(k,t)|$, could only be fitted well by $E(k,t)=\exp(-\Gamma t/2)$ at short times below a cutoff time $t_{\rm c}$, which is reported to increase with increasing system sizes.[58] Therefore, to eliminate the finite-size effect, following Refs. [58–60], we employ a restricted envelope fitting method to obtain Γ. Specifically, the appropriate short-time $E(k,t)$ data were chosen to fit to $E(k,t)=\exp(-\Gamma t/2)$ so that the data used and the fitting line could coincide.

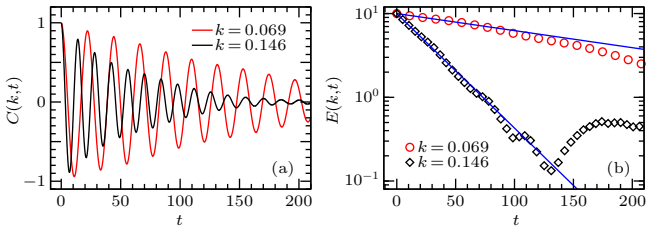


Fig. 3. Examples showing how the transverse sound attenuation coefficient Γ is determined using the restricted envelope fit method. (a) Time t evolution of the velocity correlation function $C(k,t)$ at two wavevectors $k=0.069$ and $k=0.146$. (b) The corresponding envelopes $E(k,t)$ referring to all peaks in $|C(k,t)|$. Each blue line represents a fit of the short-time data to $E(k,t)=\exp(-\Gamma t/2)$.

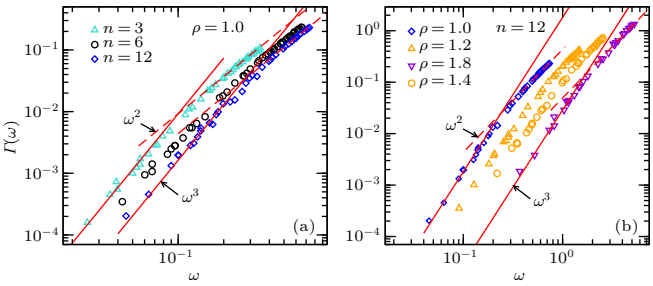


Fig. 4. Transverse sound attenuation coefficient $\Gamma(\omega)$ for the same glassy systems (with IPL interaction potentials) shown in Fig. 2. The solid and dashed red lines are the power-law scalings of $\Gamma(\omega)\sim\omega^3$ and $\Gamma(\omega)\sim\omega^2$, respectively. Note that the $\Gamma(\omega)$ data for each (n,ρ) are combined from systems with $N=20000$ and $N=100000$.

Now we are in a position to examine how the density ρ and the steepness of the interparticle repulsion χ affect the transverse sound attenuation $\Gamma(\omega)$. The χ and ρ dependences of $\Gamma(\omega)$ are shown in Figs. 4(a) and 4(b), respectively. It has been well-documented[58,60,62–64] that $\Gamma(\omega)$ follows Rayleigh scattering scaling at low frequencies within the harmonic approximation, $\Gamma(\omega)\sim\omega^{d+1}$, and hence $\Gamma(\omega)\sim\omega^3$ in 2D glasses. Moreover, $\Gamma(\omega)\sim\omega^2$ at high frequencies, regardless of spatial dimensions. For each model glass examined in Fig. 4, the low-frequency scaling of $\Gamma(\omega)\sim\omega^3$ and high-frequency scaling of $\Gamma(\omega)\sim\omega^2$ could both be observed, which thus aligns with previous conclusions. If we define $B_2=\Gamma(\omega)/\omega^2$ at high frequencies and $B_3=\Gamma(\omega)/\omega^3$ at low frequencies, it could be observed that B_3 decreases with increasing χ at fixed ρ in Fig. 4(a) or increasing ρ at fixed n in Fig. 4(b). It seems that the change of B_2 with ρ or χ has the same trend as B_3. Therefore, the strength of the sound attenuation is suppressed at all frequencies examined with an increase in the density or the steepness of interparticle repulsion. Therefore, the density and the steepness of repulsion also

share some similarity in influencing the sound attenuation besides in influencing the density of hybridized excess modes. In addition, the combination of results from Figs. 2 and 4 further supports the close connection[5,58] between the hybridized excess modes and the sound attenuation, i.e., glasses with weaker sound attenuation usually have less hybridized excess modes. However, a more quantitative characterization of the connection requires more follow-up studies.

4. Conclusion

In summary, we performed computer simulation studies of the density of excess modes hybridizing with phonon-like modes in 2D glass-formers. First, we extend the universality of the quadratic frequency dependence of the density of hybridized excess modes to a wider range of glass-formers with different interaction potentials, steepness of the repulsive interaction, and densities. The interaction potential model independence of the scaling of the density of hybridized excess modes observed here seems to be different from the proposed potential detail dependence of the density of excess modes not hybridizing with phonon-like modes.[29] This thus provides further important evidence supporting distinct properties between excess modes that do and do not hybridize with phonon-like modes.[5] Second, the connection[16] between the density of hybridized excess modes and the sound attenuation is further supported by our observations that both the density of hybridized excess modes and the strength of sound attenuation could be suppressed in glasses with a higher density or a steeper repulsion of the interaction. Further simulation work is needed to check directly in a more quantitative manner how the excess modes and sound attenuation are connected, though there have been some theoretical predictions.[4,28] Our findings indicate that the steepness of the repulsive interaction and the density share some similarities in influencing low-frequency properties of glasses. In addition, it has been reported[3,5,16,42] that glass stability could also influence the density of hybridized excess modes and the strength of sound attenuation. It would thus be interesting to check how the glass stability, density and the steepness of the repulsive interaction are interconnected in controlling low-frequency properties of glasses. Finally, it could also be necessary to check what would happen when extending the same analysis in this study to 3D glasses since the density of hybridized excess modes could depend on spatial dimensions.[3,5]

Finally, it is worth noting that we assume a power law as a good description of the low-frequency spectrum or sound attenuation, in line with what was usually done in many previous studies.[37–50] However, the available data due to current computational capacity is insufficient to confirm the accuracy of the power laws down to much lower frequencies, in particular, over several decades of frequency, which represents the big challenge inevitably encountered in recent simulation studies of low-frequency vibrations.

Acknowledgments

Project supported by the National Natural Science Foundation of China (Grant Nos. 12374202 and 12004001), Anhui Projects (Grant Nos. 2022AH020009, S020218016, and Z010118169), Hefei City (Grant No. Z020132009), and Anhui University (start-up fund). We also acknowledge Hefei Advanced Computing Center, Beijing Super Cloud Computing Center, and the High-Performance Computing Platform of Anhui University for providing computing resources.

References

[1] Kittel C 1996 *Introduction to Solid State Physics* 7th Edn. (New York: Wiley)
[2] Mizuno H, Shiba H and Ikeda A 2017 *Proc. Natl. Acad. Sci. USA* **114** E9767
[3] Wang L, Ninarello A, Guan P, Berthier L, Szamel G and Flenner E 2019 *Nat. Commun.* **10** 26
[4] Shimada M, Mizuno H and Ikeda A 2018 *Phys. Rev. E* **97** 022609
[5] Wang L, Szamel G and Flenner E 2021 *Phys. Rev. Lett.* **127** 248001
[6] Zeller R C and Pohl R O 1971 *Phys. Rev. B* **4** 2029
[7] Anderson P W, Halperin B I and Varma C M 1972 *Philos. Mag.* **25** 1
[8] Pérez-Castañeda T, Rodríguez-Tinoco C, Rodríguez-Viejo J and Ramos M A 2014 *Proc. Natl. Acad. Sci. USA* **111** 11275
[9] Xu N, Vitelli V, Liu A J and Nagel S R 2010 *Europhys. Lett.* **90** 56001
[10] Manning M L and Liu A J 2011 *Phys. Rev. Lett.* **107** 108302
[11] Xu D, Zhang S, Liu A J, Nagel S R and Xu N 2023 *Proc. Natl. Acad. Sci. USA* **120** e2304974120
[12] Widmer-Cooper A, Perry H, Harrowell P and Reichman D R 2008 *Nat. Phys.* **4** 711
[13] Chen K, Manning M L, Yunker P J, Ellenbroek W G, Zhang Z X, Liu A J and Yodh A G 2011 *Phys. Rev. Lett.* **107** 108301
[14] Wang L, Duan Y and Xu N 2012 *Soft Matter* **8** 11831
[15] Schoenholz S S, Liu A J, Riggleman R A and Rottler J 2014 *Phys. Rev. X* **4** 031014
[16] Wang L, Berthier L, Flenner E, Guan P and Szamel G 2019 *Soft Matter* **15** 7018
[17] Wang L and Xu N 2014 *Phys. Rev. Lett.* **112** 055701
[18] Zylberg J, Lerner E, Bar-Sinai E Y and Bouchbinder E 2017 *Proc. Natl. Acad. Sci. USA* **114** 7289
[19] Flenner E, Wang L and Szamel G 2020 *Soft Matter* **16** 775
[20] Tong H and Xu N 2014 *Phys. Rev. E* **90** 010401
[21] DeGiuli E, Laversanne-Finot A, Düring G, Lerner E and Wyart M 2014 *Soft Matter* **10** 5628
[22] Franz S, Parisi G, Urbani P and Zamponi F 2015 *Proc. Nat. Acad. Sci. USA* **112** 14539
[23] Buchenau U, Galperin Yu M, Gurevich V L and Schober H R 1991 *Phys. Rev. B* **43** 5039
[24] Gurevich V L, Parshin D A and Schober H R 2003 *Phys. Rev. B* **67** 094203
[25] Schober H R and Oligschleger C 1996 *Phys. Rev. B* **53** 11469
[26] Gurarie V and Chalker J T 2003 *Phys. Rev. B* **68** 134207
[27] Kumar A, Procaccia I and Singh M 2021 *Europhys. Lett.* **135** 66001
[28] Schirmacher W, Ruocco G and Scopigno T 2007 *Phys. Rev. Lett.* **98** 025501
[29] Schirmacher W, Paoluzzi M, Mocanu F C, Khomenko D, Szamel G, Zamponi F and Ruocco G 2024 *Nat. Commun.* **15** 3107
[30] Xu N, Liu A J and Nagel S R 2017 *Phys. Rev. Lett.* **119** 215502
[31] Shimada M and DeGiuli E 2022 *SciPost Phys.* **12** 090
[32] Ikeda H 2019 *Phys. Rev. E* **99** 050901
[33] Stanifer E, Morse P K, Middleton A A and Manning M L 2018 *Phys. Rev. E* **98** 042908
[34] Ji W, Popović M, de Geus T W J, Lerner E and Wyart M 2019 *Phys. Rev. E* **99** 023003

[35] Bouchbinder E, Lerner E, Rainone C, Urbani P and Zamponi F 2021 *Phys. Rev. B* **103** 174202

[36] Gartner L and Lerner E 2016 *SciPost Phys.* **1** 016

[37] Wang L, Fu L and Nie Y 2022 *J. Chem. Phys.* **157** 074502

[38] Wang L, Szamel G and Flenner E 2023 *J. Chem. Phys.* **158** 126101

[39] Lerner E and Bouchbinder E 2022 *J. Chem. Phys.* **157** 166101

[40] Lerner E, Düring G and Bouchbinder E 2016 *Phys. Rev. Lett.* **117** 035501

[41] Lerner E 2020 *Phys. Rev. E* **101** 032120

[42] Rainone C, Bouchbinder E and Lerner E 2020 *Proc. Natl. Acad. Sci. USA* **117** 5228

[43] Bonfanti S, Guerra R, Mondal C, Procaccia I and Zapperi S 2020 *Phys. Rev. Lett.* **125** 085501

[44] Richard D, González-López K, Kapteijns G, Pater R, Vaknin T, Bouchbinder E and Lerner E 2020 *Phys. Rev. Lett.* **125** 085502

[45] Kapteijns G, Bouchbinder E and Lerner E 2018 *Phys. Rev. Lett.* **121** 055501

[46] Krishnan V V, Ramola K and Karmakar S 2022 *Soft Matter* **18** 3395

[47] Paoluzzi M, Angelani L, Parisi G and Ruocco G 2019 *Phys. Rev. Lett.* **123** 155502

[48] Shiraishi K, Hara Y and Mizuno H 2022 *Phys. Rev. E* **106** 054611

[49] Shiraishi K, Mizuno H and Ikeda A 2023 *J. Chem. Phys.* **158** 174502

[50] Angelani L, Paoluzzi M, Parisi G and Ruocco G 2018 *Proc. Natl. Acad. Sci. USA* **115** 8700

[51] https://software.intel.com/en-us/mkl/

[52] Sengupta S, Vasconcelos F, Affouard F and Sastry S 2011 *J. Chem. Phys.* **135** 194503

[53] Krekelberg W P, Mittal J, Ganesan V and Truskett T M 2007 *J. Chem. Phys.* **127** 044502

[54] Zhang Z, Yunker P J, Habdas P and Yodh A G 2011 *Phys. Rev. Lett.* **107** 208303

[55] Berthier L and Tarjus G 2009 *Phys. Rev. Lett.* **103** 170601

[56] Sun X, Zhang H, Wang L, Zhang Z and Ma Y 2020 *Chin. Phys. B* **29** 126201

[57] González-López K, Shivam M, Zheng Y, Ciamarra M P and Lerner E 2021 *Phys. Rev. E* **103** 022605

[58] Wang L, Berthier L, Flenner E, Guan P and Szamel G 2019 *Soft Matter* **15** 7018

[59] Wang L, Szamel G and Flenner E 2020 *Soft Matter* **16** 7165

[60] Moriel A, Kapteijns G, Rainone C, Zylberg J, Lerner E and Bouchbinder E 2019 *J. Chem. Phys.* **151** 104503

[61] Fu L and Wang L 2022 *Phys. Rev. E* **106** 054605

[62] Szamel G and Flenner E 2022 *J. Chem. Phys.* **156** 144502

[63] Monaco G and Mossa S 2009 *Proc. Natl. Acad. Sci. USA* **106** 16907

[64] Mizuno H and Ikeda A 2018 *Phys. Rev. E* **98** 062612